The lift, drag and torque on an airfoil in foam modeled by the potential flow of a second-order fluid

J. Wang and D. D. Joseph

March, 2005

We compute the irrotational streaming flow of a second-order fluid past a Joukowski airfoil. The pressure and extra stress are evaluated using the irrotational flow theory, and the lift, drag and torque on the airfoil are obtained by integration of the normal stress over the surface of the airfoil. Our calculation can give rise to a lift force opposite to what would be predicted from the classical theory of aerodynamics. The result is in qualitative agreement with the experiments of the flow of a foam past an airfoil by Dollet, Aubouy and Graner 2004.

1 Introduction

Dollet, Aubouy and Graner [1] (hereafter referred to as DAG2004) performed experiments of the flow of a foam past an airfoil. They observed a striking feature that the lift force on the airfoil is opposite to what would be predicted from the classical theory of aerodynamics. They argued that this inverse lift is due to the effect of elasticity of the foam.

Besides the inverse lift on an airfoil, many other unusual features of flows observed in viscoelastic fluids but not in Newtonian fluids can be understood by considering the competition between the effects of inertia and viscoelasticity; for example, the stable orientation of a sedimenting long particle (Liu and Joseph [2], Galdi *et al.* [3], Wang *et al.* [4]), chaining of particles in extensional and shear flows and in sedimentation and fluidization (Michele *et al.* [5], Joseph [6], [7], chap. 7), and the two-dimensional cusp at the trailing edge of a rising air bubble (Liu, Liao and Joseph [8]). Our understanding of these phenomena relies on two pillars: a viscoelastic "pressure" generated by normal stress due to shear (Joseph and Feng [9]) and a change in the sign of the normal stress at points of stagnation (Wang and Joseph [10]). These explanations are suggested by analysis of the second-order fluid model which arises asymptotically for motions which are slow and slowly varying.

Wang and Joseph [10] considered the potential flow of a second-order fluid over a sphere or an ellipse and calculated the normal stress at the surface. The irrotational normal stress depends in a significant way on the viscosity and viscoelastic parameters and produces torques on solid particles and deformations of gas bubbles which are in qualitative agreement with experiments. The stress $\mathbf{T}$ in an incompressible second-order fluid is given by

$$\mathbf{T} = -p\mathbf{1} + \mu\mathbf{A} + \alpha_1\mathbf{B} + \alpha_2\mathbf{A}^2, \tag{1}$$

where $\mathbf{A} = \mathbf{L} + \mathbf{L}^T$ is the symmetric part of the velocity gradient $\mathbf{L} = \nabla\mathbf{u}$,

$$\mathbf{B} = \partial\mathbf{A}/\partial t + (\mathbf{u}\cdot\nabla)\,\mathbf{A} + \mathbf{A}\mathbf{L} + \mathbf{L}^T\mathbf{A}, \tag{2}$$

μ is the zero shear viscosity, $\alpha_1 = -n_1/2$ and $\alpha_2 = n_1 + n_2$ where $[n_1,\, n_2] = [N_1(\dot\gamma), N_2(\dot\gamma)]/\ \dot\gamma^2$ as $\dot\gamma \to 0$ are the constants obtained from the first and second normal stress differences.

In this work, we apply potential flow theory to the flow of a second-order fluid past an airfoil and compute the lift, drag and torque by integration of the normal stress over the surface of the airfoil. Our calculation can give the inverse lift as observed by DAG2004, but quantitative comparison between our results and the experimental ones does not yield good agreement; though foams are elastic, they are almost certainly not well described by a second-order fluid model. DAG2004 showed evidence that the inverse lift on an asymmetric object exists in a 0.5% by weight cellulose solution, which suggests that the inverse lift on an asymmetric object is a common feature in viscoelastic fluids, not only in foams. Our calculation provides a way for explicit analysis of the viscoelastic effects in such problems and offers partial explanation for the inverse lift. We regard the results using the potential flow of a second-order fluid as tentative and subject to ultimate validation by experiments and direct numerical simulation using other models.

2 Numerical method

We consider a uniform streaming flow with the velocity U_0 past a cambered airfoil at an angle of attack α. The calculation is carried out using dimensionless parameters. Following scales are used

$$[length,\ velocity,\ pressure and stress,\ time] = [l,\ U_0,\ \frac{1}{2}\rho U_0^2,\ \frac{l}{U_0}], \tag{3}$$

where l is the length of the airfoil and ρ is the density of the fluid. There are two controlling parameters in this problem:

$$R_e = \frac{\rho U_0 l}{\mu}, \quad \beta = \frac{-\alpha_1}{\rho l^2}, \tag{4}$$

where R_e is the Reynolds number and $\beta * R_e$ would give the Deborah number. Only the normal stress $T_{nn} = -p + \tau_{nn}$ at the surface is considered and the shear stress is ignored. The lift, drag and torque coefficients are defined as

$$C_L = \frac{L}{\frac{1}{2}\rho U_0^2 l}, \quad C_D = \frac{D}{\frac{1}{2}\rho U_0^2 l}, \quad C_T = \frac{T}{\frac{1}{2}\rho U_0^2 l^2}. \tag{5}$$

All the variables in the rest part of this section are dimensionless.

The airfoil is obtained by the Joukowski transformation

$$z = \zeta + \frac{c^2}{\zeta}, \tag{6}$$

in conjunction with a circle in the ζ plane. The center of the circle is displaced a distance m from the origin at an angle δ from the x axis and it is in the second quadrant (see Fig. 1). Here m is assumed to be small compared with unity. The circumference of the circle passes through the critical point $\zeta = c$ for the Joukowski transformation, which corresponds to the sharp trailing edge of the airfoil in the z plane.

In the ζ plane, a generic point (r, θ) on the circle satisfies

$$a^2 = r^2 + m^2 - 2rm\cos(\delta - \theta), \tag{7}$$

which gives rise to

$$r = m\cos(\delta - \theta) + \sqrt{a^2 - m^2\sin^2(\delta - \theta)}. \tag{8}$$

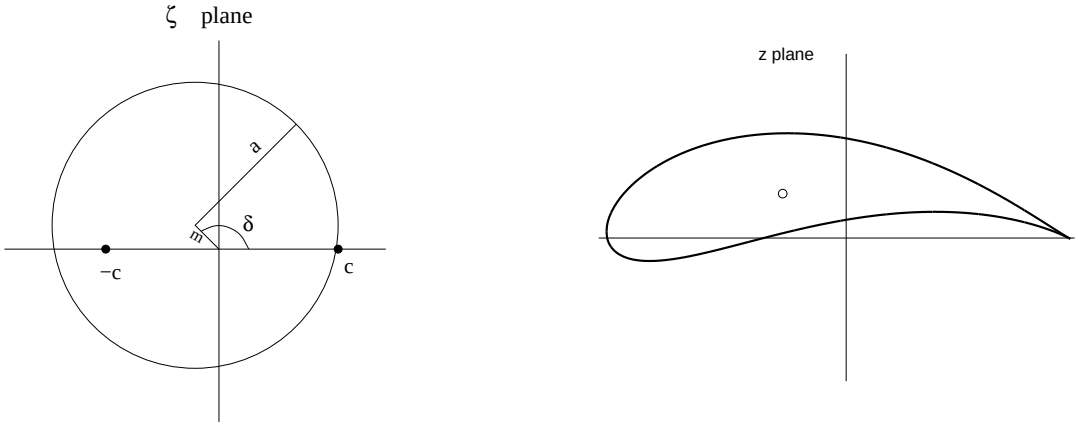

Figure 1: The mapping planes for a Joukowski airfoil. In the ζ plane, the center of the circle is displaced a distance m from the origin at an angle δ from the x axis and it is in the second quadrant. The center of the mass in the z plane $(x_0,\, y_0)$ is marked.

The critical point $(c,\, 0\,)$ is on the circle and satisfies

$$r(\theta = 0) = c = m\cos\delta + \sqrt{a^2 - m^2\sin^2\delta}. \tag{9}$$

The surface of the airfoil in the z plane is then given by

$$z = r\mathrm{e}^{\mathrm{i}\theta} + \frac{c^2}{r}\mathrm{e}^{-\mathrm{i}\theta}, \tag{10}$$

or

$$x = \left(r + \frac{c^2}{r}\right)\cos\theta \quad \text{and} \quad y = \left(r - \frac{c^2}{r}\right)\sin\theta. \tag{11}$$

The length of the airfoil can be calculated from $x(\theta = 0) - x(\theta = \pi)$ with the aid of (8) and (11):

$$1 = m\cos\delta + 3\sqrt{a^2 - m^2\sin^2\delta} + \frac{\left(m\cos\delta + \sqrt{a^2 - m^2\sin^2\delta}\right)^2}{-m\cos\delta + \sqrt{a^2 - m^2\sin^2\delta}}. \tag{12}$$

Let $\dot{x} = \mathrm{d}x/\mathrm{d}\theta$ and $\dot{y} = \mathrm{d}y/\mathrm{d}\theta$, then the unit norm on the surface pointing outward from the airfoil can be written as

$$\mathbf{n} = n_x\mathbf{e}_x + n_y\mathbf{e}_y = \frac{\dot{y}\mathbf{e}_x - \dot{x}\mathbf{e}_y}{\sqrt{\dot{x}^2 + \dot{y}^2}}, \tag{13}$$

and

$$\mathrm{d}s = \sqrt{\dot{x}^2 + \dot{y}^2}\mathrm{d}\theta. \tag{14}$$

Among the four geometric parameters c, a, m and δ, we choose to prescribe m and δ, then compute c and a from (9) and (12), respectively.

The complex potential for a uniform flow past a circle with circulation at an angle of attack α in the ζ plane is

$$f(\zeta) = \left[(\zeta - m\mathrm{e}^{\mathrm{i}\delta})\mathrm{e}^{-\mathrm{i}\alpha} + \frac{a^2\mathrm{e}^{\mathrm{i}\alpha}}{\zeta - m\mathrm{e}^{\mathrm{i}\delta}}\right] + \frac{\mathrm{i}\Gamma}{2\pi}\log\left(\frac{\zeta - m\mathrm{e}^{\mathrm{i}\delta}}{a}\right). \tag{15}$$

The circulation Γ is determined by Kutta condition, which requires $\mathrm{d}f/\mathrm{d}\zeta = 0$ at the critical point $\zeta = c$. Calculation shows that

$$\Gamma = 4\pi\left(c\sin\alpha - m\cos\delta\sin\alpha + m\sin\delta\cos\alpha\right). \tag{16}$$

Equation (15) along with the inverse Joukowski transformation

$$\zeta = \frac{z}{2} \pm \sqrt{\frac{z^2}{4} - c^2} \tag{17}$$

gives the potential for the flow past an airfoil in the z plane. The velocities can be evaluated using the potential

$$u = \frac{1}{2}\left(\frac{\mathrm{d}f}{\mathrm{d}z} + \frac{\mathrm{d}\bar{f}}{\mathrm{d}\bar{z}}\right) \quad \text{and} \quad v = \frac{\mathrm{i}}{2}\left(\frac{\mathrm{d}f}{\mathrm{d}z} - \frac{\mathrm{d}\bar{f}}{\mathrm{d}\bar{z}}\right), \tag{18}$$

where the overbar denotes conjugate variables. Wang and Joseph [10] gave the expression for the stress of a second-order fluid evaluated using a two-dimensional potential flow solution

$$\mathbf{T} = \left[-p_\infty - 1 + u^2 + v^2 + \beta(n^2 + s^2)\right]\mathbf{1} + \frac{2}{R_e}\begin{bmatrix} n & s \\ s & -n \end{bmatrix} - 2\beta u \begin{bmatrix} k & q \\ q & -k \end{bmatrix} - 2\beta v \begin{bmatrix} q & -k \\ -k & -q \end{bmatrix}, \tag{19}$$

where

$$n = \frac{\mathrm{d}^2 f}{\mathrm{d}z^2} + \frac{\mathrm{d}^2 \overline{f}}{\mathrm{d}\overline{z}^2}, \qquad s = \mathrm{i}\left(\frac{\mathrm{d}^2 f}{\mathrm{d}z^2} - \frac{\mathrm{d}^2 \overline{f}}{\mathrm{d}\overline{z}^2}\right), \tag{20}$$

$$k = \frac{\mathrm{d}^3 f}{\mathrm{d}z^3} + \frac{\mathrm{d}^3 \overline{f}}{\mathrm{d}\overline{z}^3}, \qquad q = \mathrm{i}\left(\frac{\mathrm{d}^3 f}{\mathrm{d}z^3} - \frac{\mathrm{d}^3 \overline{f}}{\mathrm{d}\overline{z}^3}\right). \tag{21}$$

The normal stress at the surface of the airfoil can be computed from

$$T_{nn} = \mathbf{n} \cdot \mathbf{T} \cdot \mathbf{n}, \tag{22}$$

where $\mathbf{n}$ is given in (13). The drag and lift coefficients are obtained by integration of T_{nn} over the airfoil surface

$$C_D = \oint T_{nn} n_x \, \mathrm{d}s, \qquad C_L = \oint T_{nn} n_y \, \mathrm{d}s. \tag{23}$$

We compute the torque with respect to the center of the mass $z = (x_0, y_0)$ by integration

$$C_T = \oint [(x - x_0)n_y - (y - y_0)n_x] T_{nn} \, \mathrm{d}s. \tag{24}$$

3 Results

We use a Joukowski airfoil described in DAG2004, which can be obtain by setting $m = 0.0911$ and $\delta = 0.688\pi$ in our calculation. The angle of attack is fixed at $\alpha = 0$, in accordance with the experiments of DAG2004. Although the velocity is finite everywhere on the airfoil surface, the velocity gradients are singular at the front nose and trailing edge (corresponding to $\theta = \pi$ and $\theta = 0$, respectively). The numerical integrations (23) and (24) cannot converge near these singular points when $\beta \neq 0$ and they have to be excluded from the integration interval. A small number Δ is introduced and the integrations are performed in the following intervals

$$0 + \Delta \leq \theta \leq \pi - \Delta, \quad \text{and} \quad \pi + \Delta \leq \theta \leq 2 * \pi - \Delta. \tag{25}$$

First we test the inviscid Newtonian fluid. Classical potential flow theory for inviscid fluid shows that the drag is zero (D'Alembert's paradox), and the lift coefficient is

$$C_L = \frac{\rho U_0 \Gamma}{\frac{1}{2}\rho U_0^2 l} = 2\frac{\Gamma}{U_0 l} = 1.90302, \tag{26}$$

where the dimensionless expression for the circulation (16) has been used for the calculation.[1] The torque on the airfoil with respect to the origin $z = 0$ can be computed using the Blasius' theorem (written in dimensionless form)

$$C_T^0 = \oint (xn_y - yn_x) T_{nn} \, \mathrm{d}s = -\mathrm{Real}\left(\oint z W^2 \, \mathrm{d}z \right) = -0.0965562, \tag{28}$$

where $W = \mathrm{d}f(z)/\mathrm{d}z$ is the complex velocity. Then the torque with respect to the center of the mass $(x_0 = -0.1362,\ y_0 = 0.0978)$can be obtained

$$\begin{aligned} C_T &= \oint (xn_y - yn_x) T_{nn} \, \mathrm{d}s - x_0 \oint n_y T_{nn} \, \mathrm{d}s + y_0 \oint n_x T_{nn} \, \mathrm{d}s \\ &= C_T^0 - x_0 C_L + y_0 C_D = 0.162651. \end{aligned} \tag{29}$$

Now we compute C_D, C_L and C_T by integration of the normal stress over the airfoil surface. The inviscid Newtonian fluid can be achieved by setting $R_e \to \infty$ and $\beta = 0$. The results are listed in the first row of Table 1 and they are in perfect agreement with the classical potential flow theory. The calculation for the inviscid fluid can converge with $\Delta = 0$; we set $\Delta = 0.05$ and repeat the calculation to test the effect of Δ. The second row of Table 1 shows that the disturbance caused by this Δ is small and C_D, C_L and C_T remain almost the same.

The total stress can be decomposed into three parts, the inertia term, the viscous term and the viscoelastic term. For an inviscid Newtonian fluid, the inertia term is the only term in the total stress. We can probe the viscous term by setting R_e to be a finite number. In the second section in Table 1, we set $R_e = 1$ and 10 and $\beta = 0$. The viscous effects lead to a positive drag, indicating that the viscous stress gives rise to a drag on the airfoil in the same direction as the incoming flow. The lift C_L increases from the value for an inviscid Newtonian fluid, showing that the viscous stress gives rise to a lift force pointing upward, in the same direction as the aerodynamic lift. The viscous stress also gives rise to a counter-clockwise torque, which is in the same direction as the torque induced by the inertia term. The viscous effects are stronger when R_e is smaller.

We set $R_e \to \infty$ and $\beta = 0.01$, 0.05 and 0.1 to suppress the viscous effects and investigate the viscoelastic effects. The third section in Table 1 shows that the viscoelastic term gives rise to a negative drag, which is opposite to the incoming flow. The viscoelastic term leads to a negative lift, which offsets the lift by inertia and gives a total lift which points downward when β is large enough. This result is in agreement with the conclusion in DAG2004 that the inverse lift is generated by viscoelasticity of the fluid. The torque due to the viscoelastic stress is clockwise, opposite to the inertia and viscous torques.

Next we consider the combined effects of the inertia term, the viscous term and the viscoelastic term. We arbitrarily set R_e from 1 to 3 and keep β to be a constant at 0.1. When $1 \le R_e \le 2.5$, the viscous contribution to C_D outweigh the viscoelastic contribution and leads to a positive drag; however, the viscoelastic contribution to C_L prevails over the viscous contribution and gives rise to a negative lift. The viscous effects attenuate as R_e increases and the viscoelastic effects become dominant. When $R_e = 3$, both C_D and C_L are negative, showing dominant viscoelastic effects. When the torque is concerned, the viscoelastic term gives the major contribution when $1 \le R_e \le 3$ and $\beta = 0.1$ and the torque is clockwise.

[1] Currie ([11], §4.18) used approximations to the first order of m and obtained another expression for the lift coefficient on the airfoil in an inviscid fluid

$$C_L = 2\pi(1 - m\cos\delta)\sin(\alpha + 4m\sin\delta) = 1.969, \tag{27}$$

which is close to the exact lift coefficient (26).

R_e	β	Δ	C_D	C_L	C_T
∞	0	0	0	1.903	0.1627
∞	0	0.05	10^{-6}	1.903	0.1626
1	0	0.05	11.674	4.288	2.670
10	0	0.05	1.167	2.141	0.4134
∞	0.01	0.05	-0.3937	1.029	-0.4167
∞	0.05	0.05	-1.969	-2.465	-2.734
∞	0.1	0.05	-3.937	-6.833	-5.630
1.0	0.1	0.05	7.737	-4.449	-3.123
1.5	0.1	0.05	3.846	-5.244	-3.959
2.0	0.1	0.05	1.900	-5.641	-4.377
2.5	0.1	0.05	0.732	-5.879	-4.627
3.0	0.1	0.05	-0.0459	-6.038	-4.795

Table 1: The lift, drag and torque coefficients on a Joukowski airfoil in the potential flow of a second-order fluid as a function of the controlling parameters R_e and β (4). The profile of the airfoil is determined by $m = 0.0911$ and $\delta = 0.688\pi$, and the angle of attack is fixed at $\alpha = 0$.

We plot the normal stress on the airfoil surface as a function of the angle θ in Fig. 2; the three curves correspond to the inviscid Newtonian fluid with $R_e = \infty$, the viscous Newtonian fluid with $R_e = 10$, and the viscoelastic fluid with $R_e = 10$ and $\beta = 0.01$, respectively. We set $p_\infty = 0$ in this calculation. The pressure is the only component of the normal stress for the inviscid Newtonian fluid. The front nose ($\theta = \pi$) is the stagnation point and the pressure gives rise to a compressive nornal stress at $\theta = \pi$. For the Newtonian fluid with $R_e = 10$, the viscous stress comes into play; Fig. 2 shows that the viscous effects make the normal stress more compressive at the stagnation point. For the viscoelastic fluid with $R_e = 10$ and $\beta = 0.01$, the normal stress varies dramatically near the stagnation point. Although we cannot compute the normal stress precisely at $\theta = \pi$ because it is singular, we can compute points close to $\theta = \pi$ and connect them to obtain a curve. The curve in Fig. 2 shows that T_{nn} becomes tensile near $\theta = \pi$ due to the viscoelastic effects. This change of sign of the normal stress at the stagnation point plays a role in the inverse lift force on the airfoil; it also has significant importance in many unusual features in viscoelastic fluids, such as the stable orientation of a sedimenting long particle, chaining of particles in extensional and shear flows, and the cusp at the trailing edge of a rising air bubble (Wang and Joseph [10]).

DAG2004 measured the drag and lift on an airfoil in the streaming flow of a foam. The drag is in the same direction as the streaming flow; the lift is in the opposite direction to what would be predicted from the theory of aerodynamics. Compared to our calculation, their experiments correspond to the regime in which the viscous contribution prevails for the drag, whereas the viscoelastic contribution prevails for the lift. In Figure 3 the lift and drag coefficients measured by DAG2004 are plotted against the Reynolds number.

Our calculation cannot reproduce the experimental results of DAG2004 shown in Figure 3 quantitatively. The parameter β for the foam used in the experiments is not known. We cannot find a value of β which leads to good agreement between our calculation and the experimental results. Part of the reason may be due to the fact that the experiments of DAG2004 are in low Reynolds number ($R_e \sim 0.1$) regime and the yield stress of the foam plays an important role, which is not accounted for in the second-order fluid model. Nevertheless, our calculation can correctly predict the directions of the drag and lift and is an improvement on the inviscid potential flow theory in aerodynamics.

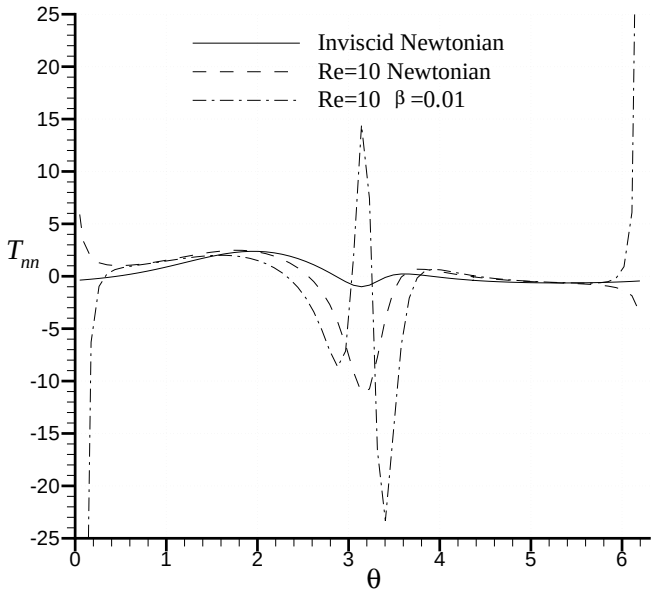

Figure 2: The normal stress on the airfoil surface as a function of the angle θ. The solid line corresponds to the inviscid Newtonian fluid with $R_e = \infty$, the dashed line to the viscous Newtonian fluid with $R_e = 10$, and the dash-dotted line to the viscoelastic fluid with $R_e = 10$ and $\beta = 0.01$.

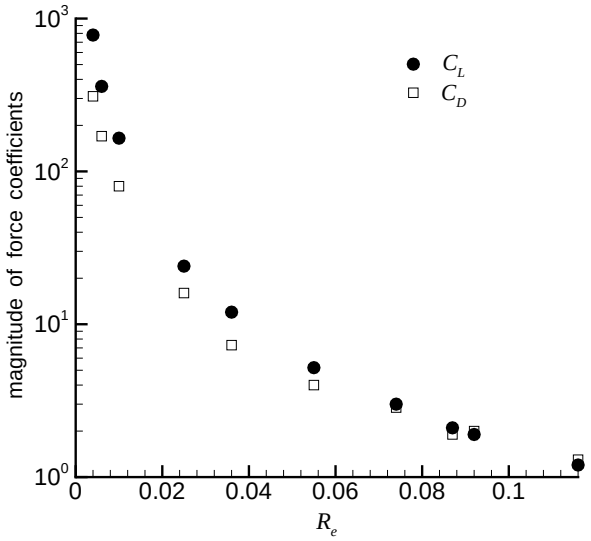

Figure 3: The magnitude of C_L and C_D on an airfoil in the flow of a foam measured by DAG2004 against the Reynolds number. The drag is in the uniform flow direction; the direction of the lift force is opposite to what would be predicted from the theory of aerodynamics.

Potential flow of a second-order fluid provides an explicit and effective way of analyzing viscoelastic effects in simple flows.

Acknowledgments

This work was supported in part by the NSF under grants from Chemical Transport Systems. We are thankful to B. Dollet, M. Aubouy and F. Graner for showing their results to us and for enlightening discussions.

References

[1] Dollet B., Aubouy M. and Graner F. 2004 Inverse lift in a flowing foam. Submitted.

[2] Liu, Y. J. and Joseph, D. D. 1993 Sedimentation of particles in polymer solutions. *J. Fluid Mech.*, **255**, 565–595.

[3] Galdi, G. P., Pokomy, M., Vaidya, A., Joseph, D. D. and Feng, J. 2002 Orientation of symmetric bodies falling in a second-order liquid at non-zero Reynolds number. *Math. Models Methods Appl. Sci.* **12**(11), 1653 – 1690.

[4] Wang, J., Bai, R., Lewandowski, C., Galdi, G. P. and Joseph, D. D. 2004 Sedimentation of cylindrical particles in a viscoelastic liquid: shape-tilting. *China Particuology*, **2**(1), 13 – 18.

[5] Michele, J., Päzold, R. and Donis, R. 1977 Alignment and aggregation effects in suspensions of spheres in non-Newtonian media. *Rheol. Acta.* **16**, 317 – 321.

[6] Joseph, D. D. 1996 Flow induced microstructure in Newtonian and viscoelastic fluids. In *Proc. 5^{th} World Congress of Chem. Eng., Particle Technology Track, San Diego.* July 14-18. AICHE **6**, 3–16.

[7] Joseph, D. D. 2000 *Interrogation of direct numerical simulation of solid-liquid flow*, available at http://www.efluids.com/efluids/books/joseph.htm.

[8] Liu, Y. J., Liao, T. Y. and Joseph, D. D. 1995 A two-dimensional cusp at the trailing edge of an air bubble rising in a viscoelastic liquid. *J. Fluid Mech.*, **304**, 321–342.

[9] Joseph, D. D. and Feng, J. 1996 A note on the forces that move particles in a second-order fluid. *J. Non-Newt. Fluid. Mech.* **64**, 299–302.

[10] Wang, J. and Joseph D. D. 2004 Potential flow of a second-order fluid over a sphere or an ellipse. *J. Fluid Mech.* **511**, 201 – 215.

[11] Currie, I. G. 1974 *Fundamental Mechanics of Fluids*, McGraw-Hill, Inc.